RSC Advances

PAPER

View Article Online
View Journal | View Issue

Cite this: *RSC Adv.*, 2023, **13**, 6160

Immobilized Cu(0) nanoparticles on montmorillonite-modified with benzalkonium chloride (MMT-BAC@Cu(0)): as an eco-friendly and proficient heterogeneous nano-catalyst for green synthesis of 5-substituted 1*H*-tetrazoles†

Fatemeh Pirani,[a] Hossein Eshghi *[a] and S. Amin Rounaghi [b]

Received 24th December 2022
Accepted 1st February 2023

DOI: 10.1039/d2ra08208j

rsc.li/rsc-advances

In this study, Cu(0) nanoparticles supported on organo-modified montmorillonite with benzalkonium chloride (MMT-BAC@Cu(0)) were synthesized and used as an eco-friendly and green heterogeneous catalyst for the synthesis of 5-substituted 1*H*-tetrazoles in mild media. The structure of the catalyst was investigated using various techniques including XRD, EDX, ICP, TEM, FE-SEM, and FT-IR. The advantages of availability, low cost, non-toxicity, and biocompatibility of clay were our focus in synthesizing this nanoclay catalyst. The method's advantages include good to excellent product yields, mild conditions, easy work-up, short reaction times, and easy reuse of the nanocatalyst.

Introduction

A recent focus has come on using clay minerals as heterogeneous and green catalysts.[1] In this regard, montmorillonite (MMT) clay has drawn particular attention due to its high abundance, cation exchange capacity, and other surface areas. The montmorillonite (MMT) clay soil with the general formula $(Al_{2-x}Mg_x)\ Si_4O_{10}(OH)_2\cdot(M\cdot nH_2O)$ belongs to the family of phyllosilicates (2 : 1), containing two tetrahedral planes and an octahedral plane. Some highly developed applications of clay minerals because of their properties such as biocompatibility, abundance, inexpensiveness, and harmless to health include their uses in cosmetics, pharmacology, and nanocomposites.[2,3] The use of MMT clay has been reported for removing organic pollutants due to its high and excellent adsorption capacity. The organic adsorption capacities are attributed to its multilayer structure. The surfaces of MMT clay possess negative charges because Si and Al in the MMT clay are probably substituted with Ca, Mg, K, Na, and other elements. Moreover, low-capacity metal cations can also diffuse into the intermediate layers of MMT clay. MMT clay is one of the proper supports in which metal nanoparticles can be fixed on the spaces between the layers or inside the pores. The synthesis and applications of clay nanoparticles in catalysis is a newfound and emerging field. The MMT clay benefitting from high dispersion, excellent charge trapping, remarkable absorption capacity, and high sustainability. Properties such as cation exchange capacity, high surface reactivity, high adsorption capacity, biocompatibility, uses in cosmetics, catalysis, pharmacy, medicine, and sensors can be named as some MMT clay applications.[4,5] Because of their adjustable Brønsted and Lewis acidities, clays are utilized as effective catalysts for various organic transformations.[6,7]

Many natural remedies and medicines such as atropine, codeine, morphine, diazepam, metronidazole, azidothymidine, and methotrexate are known as heterocyclic compounds.[8,9] Some major goals of organic chemistry and medicine appear to be the design, synthesis, and production of valuable molecules as human therapeutic agents.[10–12] Tetrazoles are known as another major class of synthetic heterocyclic compounds with highly significant medicinal properties. Tetrazoles and their derivatives have drawn much attention in designing drugs as bioactive compounds[13,14] (Fig. 1). Thus, it is no wonder that the synthesis of tetrazoles has turned into a hot topic in the organic field so dramatically that it has drawn huge focus and attention in academic research and industrial areas.

It is interesting to know that there are few reports regarding the use of the multi-component domino reactions between aldehydes, malononitrile, and sodium azide to synthesize 2-(1*H*-tetrazole-5-yl) acrylonitrile derivatives.[15–17] These reactions were carried out by using various catalysts, according to the reports.[18–23] Despite their usefulness, some of these methods suffer from several disadvantages, such as long reaction times, expensive and toxic reagents, and difficulty in separating and reusing the catalyst. Moreover, many catalysts need to use dimethylformamide (DMF) as a solvent during the reaction,

[a]*Department of Chemistry, Faculty of Science, Ferdowsi University of Mashhad, Mashhad 91775-1436, Iran. E-mail: heshghi@um.ac.ir*

[b]*Research and Development Laboratory, Nano Parmin Khavaran Company, Birjand, Iran*

† Electronic supplementary information (ESI) available. See DOI: https://doi.org/10.1039/d2ra08208j

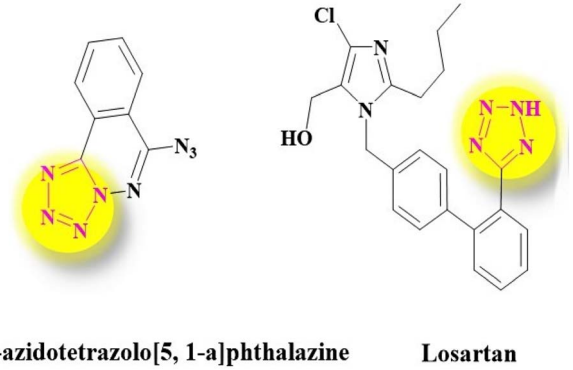

Fig. 1 Two bioactive molecules containing the tetrazole core.

while the green chemistry[24] perspective insistently looks forward to developing safe and clean processes in the presence of solvents and green catalysts.[25–29] Thus, choosing a proper catalyst and green solvent for each reaction is crucial to obtain perfect results.[30] Furthermore, reports reveal that copper may be effective in the synthesis of beneficial organic compounds as catalysts,[31,32] such as in the synthesis of tetrazoles.[33,34] Because of its lower cost, copper has been utilized in the structure of various catalysts.[35,36]

This study aimed to develop a biocompatible nanocatalyst based on immobilized Cu(0) nanoparticles on montmorillonite-modified with benzalkonium chloride (MMT-BAC@Cu(0)) for the synthesis of 5-substituted-1*H*-tetrazoles under mild and green conditions (Scheme 1).

Results and discussion

Characterization of the immobilized Cu(0) nanoparticles on montmorillonite-modified with benzalkonium chloride (MMT-BAC@Cu(0)) nanoclay. To synthesize the nanocatalyst, an aqueous solution of $Cu(NO_3)_2 \cdot 6H_2O$ was added to MMT-BAC, and the resulting mixture was stirred at 80 °C at a high and uniform speed. Then, $NaBH_4$ was added to form Cu nanoparticles (Scheme 2).

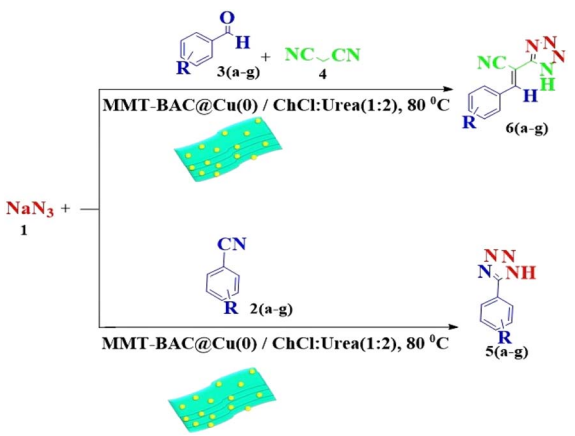

Scheme 1 Synthesis of 5-substituted-1*H*-tetrazoles.

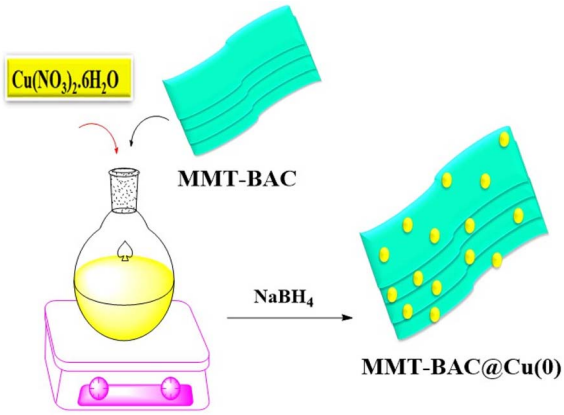

Scheme 2 Schematic representation of the synthesis of MMT-BAC@Cu(0)nano catalyst.

Finally, the obtained catalyst (MMT-BAC@Cu(0)) was dried and characterized by XRD, FT-IR, FE-SEM, EDX, ICP, and TEM techniques.

Structure, elemental, and morphology of the MMT-BAC@Cu(0)

FT-IR spectroscopy was performed to confirm the chemical structure of the synthesized catalyst. The FT-IR spectra of (a) MMT-BAC and (b) MMT-BAC@Cu(0) samples are shown in Fig. 2. In the case of MMT-BAC, the peaks at 1034, 914, and 791 cm^{-1} can be concertedly attributed to the stretching vibrations of Si–O in Si–O–Al, and bending vibration modes of Al–Al–OH and Mg–Mg–OH groups, respectively.[1] The spectrum of MMT-BAC showed two strong bands at 3620 and 1034 cm^{-1} that corresponds to the clay and O–H stretching vibration modes of the structural OH groups. The O–H stretching mode of the interlayer water appears at 3405 cm^{-1} and the H–O–H bending mode of the adsorbed water at 1644 cm^{-1}. The FT-IR spectrum of BAC shows a set of bands at 2925 and 2852 cm^{-1} corresponding to the CH_2 (asymmetric and symmetric stretching modes, respectively). The bands at 1468 and 1456 cm^{-1} are assigned to the CH_2 scissoring modes and the band at 730 cm^{-1} can be attributed to the CH_2 rocking mode.

The FT-IR spectrum of MMT-BAC@Cu(0) shows typical main bands at 3624, 3442, 1632, 1037, 910, and 517 cm^{-1}. The strong band at 1037 cm^{-1} is also assigned to the Si–O stretching vibration of the tetrahedral sites. A small band around 792 cm^{-1} is assigned to amorphous silica, and the bands at 517 cm^{-1} and 465 cm^{-1} are attributed to the bending vibration of Si–O–Al and Si–O–Si bonds.[37] The Cu–O peaks are likely to appear at 623 and 465.[38] The peaks related to Cu–O overlap with the clay peaks in the FT-IR spectrum. Comparing the FT-IR spectra of (a) MMT-BAC, (b) MMT-BAC@Cu(0), (c) MMT-BAC@Cu(0) (fresh catalyst), and (d) the recycled MMT-BAC@Cu(0) nanocatalyst after five times MNPs with that of MMT-BAC shows that no recognizable changes, because of the overlapping of absorption bands, are observable in the FT-IR spectra (Fig. 2).

XRD analysis was performed to obtain information about the crystallographic structure of the catalyst (Fig. 3). The typical

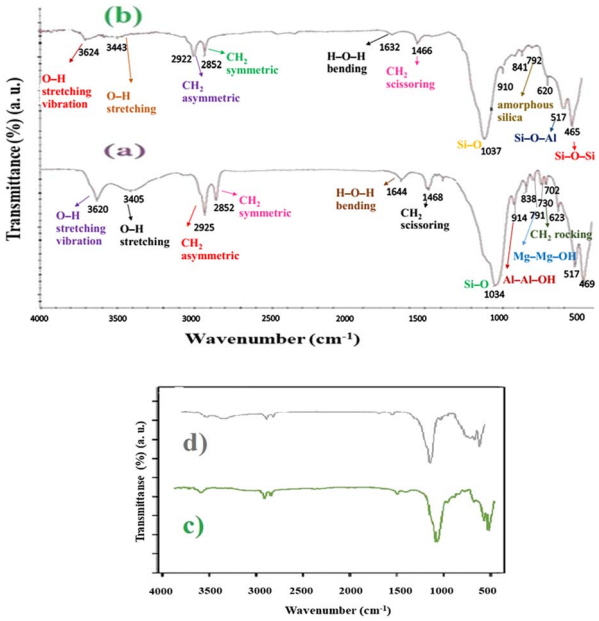

Fig. 2 FT-IR spectra. (a) MMT-BAC and (b) MMT-BAC@Cu(0) (up) and the comparing FT-IR spectra of (c) fresh catalyst and (d) recycled catalyst (down).

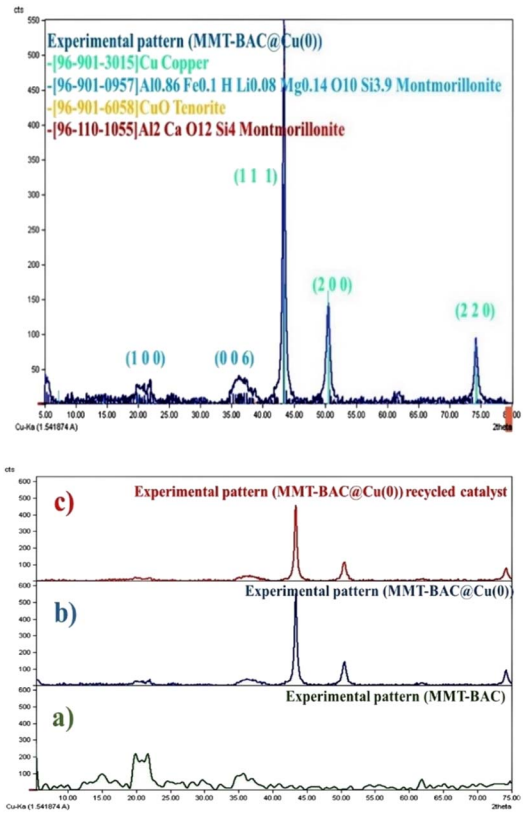

Fig. 3 XRD pattern of MMT-BAC@Cu(0) nanoclay (up) and the comparing XRD pattern of (a) MMT-BAC, (b) MMT-BAC@Cu(0), (c) recycled catalyst (down).

XRD pattern contains several peaks that are clearly distinguishable and represents the diffraction pattern of Cu nanoparticles in which the peaks at 2θ values of 43.30°, 50.44°, and 74.82° corresponding to (111), (200), and (220) planes, respectively.[39]

The appeared peaks at $2\theta = 19.9°$ (100) and 35.7° (006) indicate the immobilization of Cu nanoparticles into the interlamellar spaces of clay mineral. In the XRD profile, the observed peaks are related to Cu nanoparticles, and the reduction is well done. Furthermore, some other peaks are seen in the XRD image of the sample in addition to metallic copper, which is probably related to monovalent copper oxide (the high percentage of oxygen on the sample surface in EDX images is probably related to this compound as well as the surface oxide of copper nanoparticles). The volume of the copper raw material in the reaction was high, which saturated the surfaces of the clay planes and then created coarser copper particles on the clay layers. The XRD pattern of the recycled catalyst is similar to that of the fresh catalyst, indicating the good performance of the catalyst (Fig. 3).

Ca, K, Mn, and Al are the major constituents of clay. MMT-BAC@Cu(0) nanoclay contains a high copper concentration (based on the ICP analysis), which has probably caused copper particles to be formed excessively as separate agglomerates (Table 1).

The EDX spectrum of MMT-BAC@Cu(0) indicates several elements, such as C, N, O, Si, Mg, Al, and Cu (Fig. 4). EDX images also represent the distribution of copper and silica throughout the sample image. However, the EDX elemental analysis also reveals a very high percentage of copper compared to other elements, which is mainly due to the high amount of copper raw material used during synthesis. On the other hand, copper particles cover the surface of the clay planes. Thus, a weaker signal was received from the underlying nano-clay layers (Si and Al). As shown in Fig. 5, the elemental mapping of Al, Mg, Cu, N, O, Cl, Si, and O confirmed the uniform distribution of the nanocatalyst components.

The surface morphology and particle sizes of the synthesized MMT-BAC@Cu(0) catalysts were determined using FE-SEM. As seen in Fig. 6, many copper particles are formed as relatively large agglomerates, which have covered the nanoclay planes. Some particles in the sample seem to be positioned separately and mixed with nanoclay planes with no uniform distribution. In addition, the samples of rod particles can be seen in Fig. 6, probably related to the formation of different morphologies of copper particles. Although no chemical linkers are used during synthesis, the adsorption of nanoparticles on nanoclay plates in this sample may be resulting from either the interaction between the nanoclay planes with the metal or the simultaneous interaction of the ammonium benzalkonium head attached to the clay surface with the surfaces of metal particles (Fig. 6).

The particles can be seen on the edge of the clay planes in the TEM images at high magnification (Fig. 7). The coating process

Table 1 ICP analysis of MMT-BAC@Cu(0) nanoclay

Elements	Ca	K	Mn	Al	Cu
Reported [ppm]	2373	4111	2251	19 626	493 383

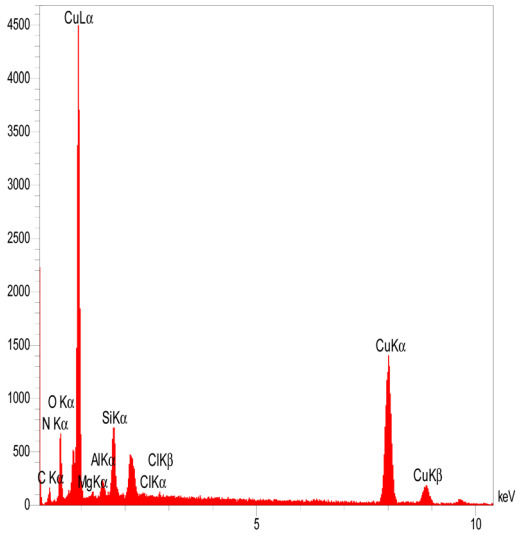

Fig. 4 EDS diagram of MMT-BAC@Cu(0) nanoclay.

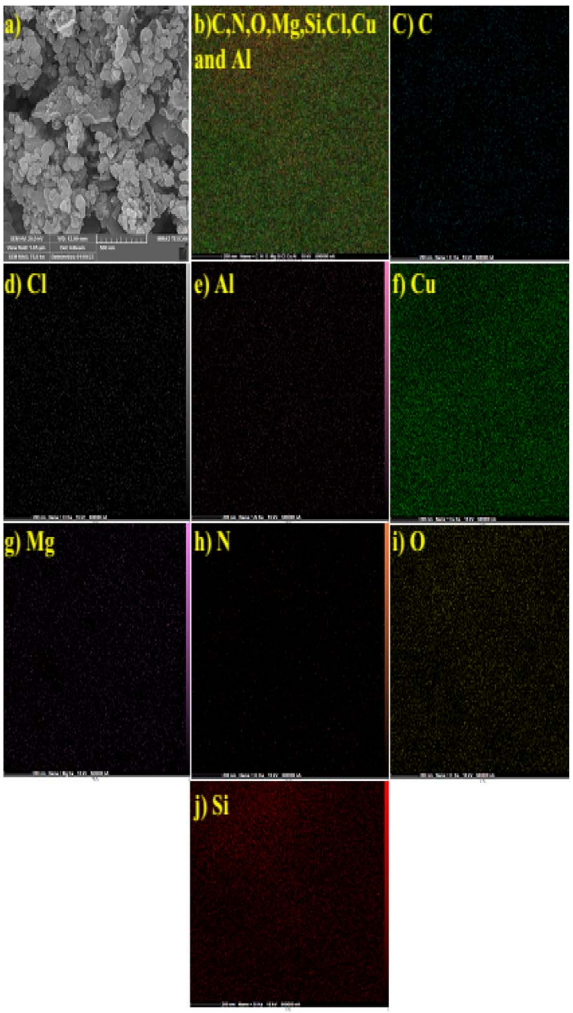

Fig. 5 Elemental mapping of MMT-BAC@Cu(0) nanoclay. (a) Selected SEM image, (b) C, N, O, Mg, Si, Cl, Cu and Al, (c) C, (d) Cl, (e) Al, (f) Cu, (g) Mg, (h) N, (i) O and (j) Si.

of the surface of the clay planes with copper seems to have proceeded well since the particles have been placed just on the planes, and no blank clay plane or individual particles are observed. We may describe two possibilities to explain the dark areas on the planes. These areas have multiple clay layers (unlike the sides, mostly monolayers). Thus, these areas appear to be dark because of the presence of several layers and the coating of each layer with copper nanoparticles (which is a heavy metal). The volume of the copper raw material in the reaction was high, which saturated the surfaces of the clay planes and then created coarser copper particles on the clay layers. At higher image magnifications, it was revealed that the dark areas are mostly composed of nanometer-sized particles next to each other (rather than integrated particles). Benzalkonium is located between the clay planes, and its ammonium head is placed in front of the plane's surface. This molecule is evenly distributed on the surface of the clay planes. The highly uniform distribution of copper particles embedded only on the clay (no discrete copper particles are observed) supports the hypothesis that benzalkonium molecules play a crucial role in the preferential formation of copper nanoparticles on the clay platelets.

Application of the MMT-BAC@Cu(0) for the synthesis of 5-substituted-1*H*-tetrazoles

The reaction of sodium azide with benzonitrile was considered the model reaction to optimize the conditions in the synthesis of 5-substituted 1*H*-tetrazole derivatives. Initially, different solvents, such as H_2O, EtOH, DMF, organic solvents, and several different deep eutectic solvents (DESs) were used to provide optimal conditions in that the best result was associated with DES. Then, different amounts of DES and MMT-BAC@Cu(0) nanocatalysts were tested at several different temperatures. The point is that the catalyst disperses better in the DES (ChCl :

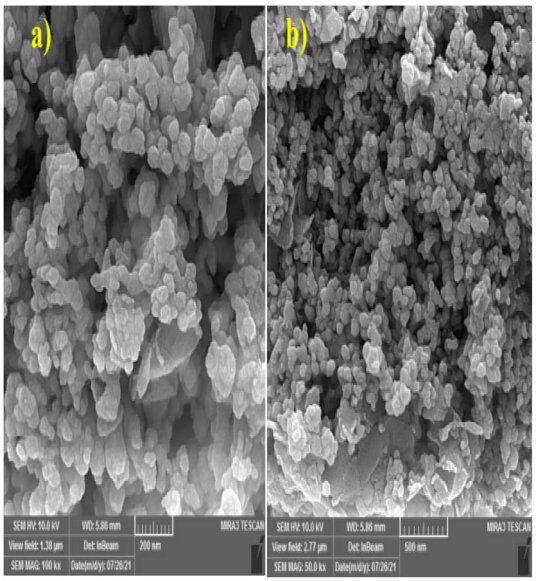

Fig. 6 FE-SEM image of MMT-BAC@Cu(0) nanoclay (a and b) in different resolutions.

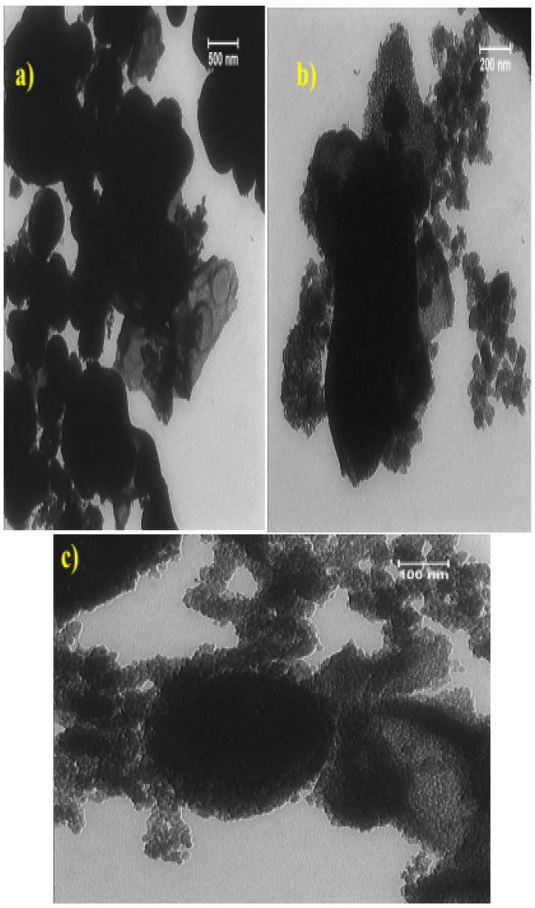

Fig. 7 TEM image of MMT-BAC@Cu(0) nanoclay (a–c) in different resolutions.

urea, 1 : 2) and this leads to a good performance of the catalyst under mild conditions.

The best results were obtained at 80 °C, 0.5 g of DES, (choline chloride (1.0 mmol) and urea (2.0 mmol)) (ChCl : urea, 1 : 2), and 0.015 g of MMT-BAC@Cu(0) as the catalyst (Table 2).

According to the following observations (Table 3, entries 1–7), in the synthesis of 5-substituted 1*H*-tetrazole derivatives from benzonitrile derivatives and sodium azide, the activity of the nitrile compound relative to the azide ion plays a vital role in this cycloaddition reaction. Accordingly, different benzonitrile derivatives containing electron-releasing groups (ERG) react faster than benzonitriles containing EWGs, and products with higher efficiencies are obtained in shorter reaction times. If benzonitrile containing an electron-withdrawing group is used (*p*-NO_2–benzonitrile), the reaction fails even for a long reaction time (12 h). The reason is that the electron-releasing groups resonate with the nitrile group, and facilitate a better activation with the Cu nanocatalyst. Also, the raw materials, benzaldehydes, malononitrile, and sodium azide were used to synthesize 1*H*-tetrazole derivatives (entries 8–13). Various substitutions, including electron-releasing and withdrawing groups, were tested to evaluate the scope and limitations of this method. The electron-releasing and withdrawing groups did not cause significant differences in product yields and the reaction time through multicomponent domino reactions (MDRs) to form products under mild and green conditions (Table 3). Interestingly, in this multicomponent domino reaction, benzaldehyde containing electron withdrawing group (*m*-NO_2–benzaldehyde) produced the corresponding product in high yield. Since the related benzylidine malononitrile contains two different nitrile groups and one of them is affected by an electron-withdrawing group and the other can be activated with a nanocatalyst.

All the products were characterized by comparing their melting points with those reported in the literature[16,17,20,40–42] and NMR spectroscopy (see ESI†). The catalytic performance of MMT-BAC@Cu(0) and the use of DES as a green solvent were compared with some previously reported methods to evaluate the present protocol according to other reported 5-substituted 1*H*-tetrazole derivatives synthesis methods.

According to Table 4, although all the methods were useful, still, many of them have several drawbacks, including hazardous and volatile organic solvents, long reaction times, and low efficiencies. However, preparing 5-substituted 1*H*-tetrazole derivatives using a biocompatible MMT-BAC@Cu(0) nanocatalyst in the presence of DESs provided high yields. We found a high efficiency under mild conditions and lower temperatures and shorter reaction times. The conditions were moderate and green in the case of the catalyst and solvent (Table 4).

Proposed mechanism for the synthesis of a 5-substituted 1*H*-tetrazole derivative

The reaction involves [3 + 2] cycloaddition between benzonitrile and sodium azide. The applied conditions include the use of DES and MMT-BAC@Cu(0) nanocatalyst. A proposed mechanism could involve the covering role of DES that could activate the dipoles in the medium and activate and strengthen the electrophilic parts for the nucleophilic attack by establishing hydrogen bonding. MMT-BAC@Cu(0) also modified benzalkonium on the surface, making an effective interaction (π–π) with the aromatic ring of the substrates. The Cu nanoparticle can also interact with CN and make it more active. In general, it facilitates the attack of benzonitrile and sodium azide through the [3 + 2] cycloaddition reaction. Finally, the product of 5-substituted 1*H*-tetrazoles was formed (Fig. 8). In the cases of other synthesized 5-substituted 1*H*-tetrazoles, the related benzylidene malononitrile, which was obtained *in situ* from the reaction of benzaldehyde and malononitrile, contains two different nitrile groups, and one of them affected the electron-withdrawing group and other can be activated with the nanocatalyst (Fig. 8).

Recycling of MMT-BAC@Cu nanocatalyst

The reusability of MMT-BAC@Cu(0) nanocatalyst was examined in [2 + 3] cycloaddition between benzonitrile (1.0 mmol) and sodium azide (1.0 mmol) in DES as the green reaction medium. The reaction was performed using MMT-BAC@Cu(0) nanocatalyst (0.015 g) (Fig. 9). After the reaction was complete, the recovered MMT-BAC@Cu(0) nanocatalyst was washed several times with hot ethanol and then dried at 50 °C for 16 h. We

Table 2 Optimization of reaction conditions for the synthesis of 5-phenyl-1*H*-tetrazole

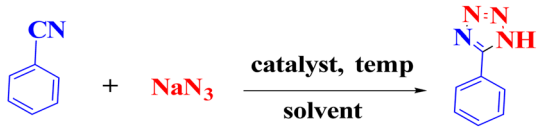

Entry	Catalyst[a] (g)	Solvent	Temp. (°C)	Time (h)	Yield[b] (%)
1	—	—	110	20	—
2	—	H_2O	Reflux	26	—
3	0.015	H_2O	Reflux	7	58
4	0.015	DMF	110	6	87
5	0.015	EtOH	Reflux	7	48
6	0.015	ChCl : urea (1 : 2) (0.5 g)	80	0.5	99
7	0.015	ChCl : urea (1 : 2) (1 g)	100	1	98
8	0.015	ChCl : urea (1 : 2) (1 g)	80	1	98
9	0.015	ChCl : Gly (1 : 4) (0.5 g)	90	1	99
10	0.015	ChCl : ethylene glycol (1 : 4) (0.5 g)	100	2	97
11	0.015	ChCl : urea (1 : 2) (0.5 g)	90	0.5	99
12	0.02	ChCl : urea (1 : 2) (0.5 g)	80	0.5	99
13	0.008	ChCl : urea (1 : 2) (0.5 g)	80	1.5	90

[a] MMT-BAC@Cu(0) nanocatalyst was used with 1.0 mmol of the substrates. [b] Isolated yield.

observed that the recovered MMT-BAC@Cu(0) nanocatalyst could be used for five successive runs. A comparison of the FT-IR spectra of the fresh MMT-BAC@Cu(0) and recovered one after using it five times in the reaction is shown in Fig. 2. In addition, XRD analysis of the recycled MMT-BAC@Cu(0), as shown in Fig. 3 proves that it has no obvious change in its structure after five times recovery.

Experimental

General

All reagents were purchased from Merck and Fluka and used without further purification. Organo-modified montmorillonite with benzalkonium chloride was supplied by Nano parmin Khavaran company. The melting points were recorded on an Electro thermal type 9100 melting point apparatus. The FT-IR spectra were recorded on Avatar370 FT-IR Thermo Nicolet, and only noteworthy absorptions are mentioned. The ^{1}H NMR (300 MHz) and the ^{13}C NMR (75 MHz) spectra were recorded on a Brucker DRX-300 Avance, using (DMSO-d_6) as the solvent and TMS as the internal standard at 300 and 75 MHz, respectively; δ in ppm, J in Hz. The mass spectra were scanned on a Varian Mat CH-7 at 70 eV. The size and morphology of the prepared catalysts were studied using TEM (a Leo 912AB microscope operated at 120 kV) and FESEM (TESCAN BRNO-Mira3 LMU). The metal loading and leaching were evaluated with ICP-OES analyses (an Avio 200 ICP Optical Emission Spectrometer).

Preparation of immobilized Cu(0) nanoparticles on montmorillonite-modified with benzalkonium chloride (MMT-BAC@Cu(0))

$Cu(NO_3)_2 \cdot 6H_2O$ (100 mL, 0.05 M) aqueous solution was added to MMT-BAC (0.5 g). The resulting mixture was stirred at 80 °C for 8 hours at a high and uniform speed. Then, $NaBH_4$ (34.0 mmol, 1.32 g) was added. Finally, the resulting mixture was washed several times with deionized water and ethanol after filtering. Then, the resultant precipitation was dried for 14 hours at 50 °C in a vacuum oven, and finally, the catalyst MMT-BAC@Cu(0) was obtained.

Preparation of DES

DES (ChCl : urea) (1 : 2) were prepared using the method described by Abbott *et al.*[48] Choline chloride (1.0 mmol, 0.139 g) and urea (2.0 mmol, 0.120 g) were mixed together and heated at 50 °C until a clear homogeneous liquid was formed.

A typical procedure for the preparation of the 5-substituted 1*H*-tetrazole derivatives (5a–g)

Benzonitriles (**2a–g**) (1.0 mmol) and sodium azide (1.0 mmol, 0.065 g), and MMT-BAC@Cu(0) nanocatalyst (0.015 g) in DES (ChCl : urea of 1 : 2) (0.5 g) was magnetically stirred at 80 °C for a specified time (see Table 3). The reaction progress was monitored by TLC. Upon completion of the reaction, the reaction mixture was cooled to ambient temperature, and deionized water (5 mL) was added and stirred for 1 hour. After the separation of the catalyst by filtration, hydrochloric acid solution (10 mL, 5 N) was added to the filtrate solution, and the precipitated tetrazole was filtered and recrystallized from ethanol.

A typical procedure for the preparation of the 5-substituted 1*H*-tetrazole derivatives (6a–g)

Aldehydes (**3a–g**) (1.0 mmol), malononitrile (1.0 mmol, 0.066 g), and sodium azide (1.0 mmol, 0.065 g), and MMT-BAC@Cu(0) nanoclay (0.015 g) in DES (ChCl : urea, 1 : 2) (0.5 g) was magnetically stirred at 80 °C for a specified time (see Table 3).

Table 3 The synthesis of 5-substituted 1*H*-tetrazoles derivatives using the MMT-BAC@Cu(0) nanoclay in ChCl : urea (1 : 2)[a]

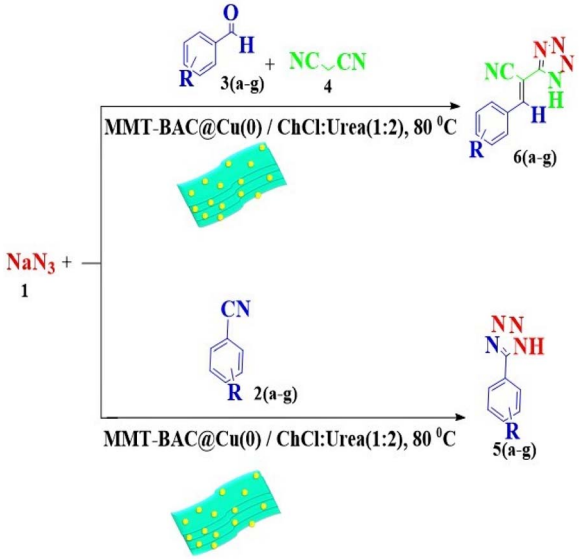

Entry	Product	Time (min)	Yield[b] (%)	M.p.[c] (°C) (ref.)
1	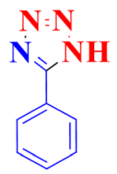 5a	30	99	214–215 (ref. 40)
2	 5b	50	96	150–151 (ref. 20)
3	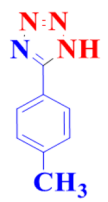 5c	60	96	250–251 (ref. 20)
4	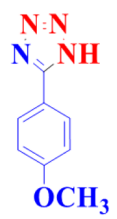 5d	45	94	229–230 (ref. 20)

Table 3 (*Contd.*)

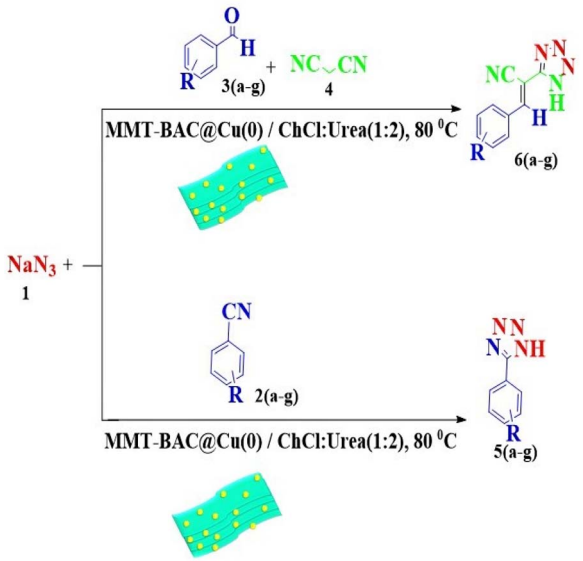

Entry	Product	Time (min)	Yield[b] (%)	M.p.[c] (°C) (ref.)
5	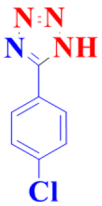 5e	25	99	260–261 (ref. 20)
6	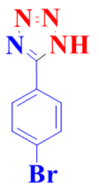 5f	35	98	265–267 (ref. 20)
7	 5g	80	95	172–173 (ref. 41)
8	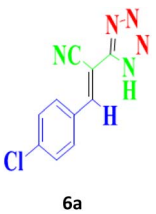 6a	120	90	166–168 (ref. 16)

Table 3 (*Contd.*)

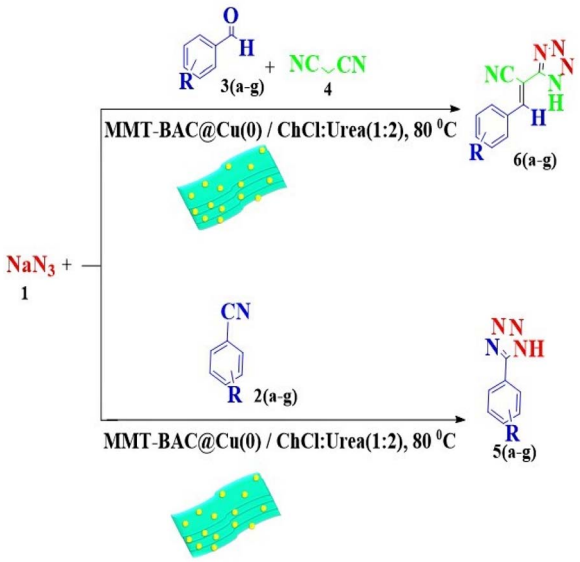

Entry	Product	Time (min)	Yield[b] (%)	M.p.[c] (°C) (ref.)
9	 6b	120	95	160–162 (ref. 42)
10	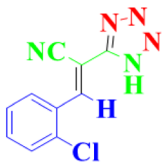 6c	90	97	176–178 (ref. 16)
11	 6d	120	98	166–169 (ref. 42)
12	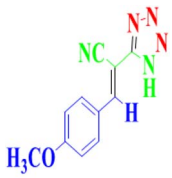 6e	180	94	152–154 (ref. 17)

Table 3 (*Contd.*)

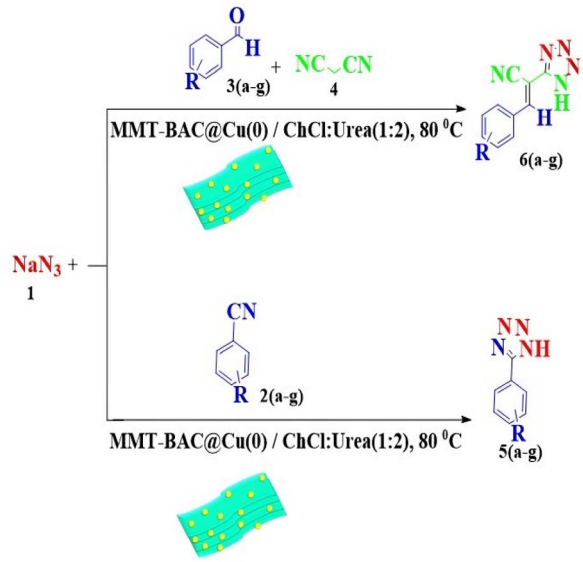

Entry	Product	Time (min)	Yield[b] (%)	M.p.[c] (°C) (ref.)
13	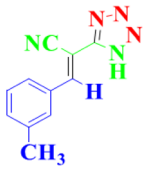 6f	240	88	131–133 (ref. 17)

[a] Reaction conditions: aldehydes (**3a–g**) (1.0 mmol), benzonitriles (**2a–g**) (1.0 mmol), malononitrile (1.0 mmol, 0.066 g), and sodium azide (1.0 mmol, 0.065 g), and MMT-BAC@Cu(0) nanoclay (0.015 g) in DES (ChCl : urea) (1 : 2) (0.5 g). [b] Isolated yield. [c] Melting points and spectroscopic data were compared with the literature.

The reaction progress was monitored by TLC. Upon completion of the reaction, the reaction mixture was cooled to ambient temperature, and deionized water (5 mL) was added and stirred for 1 hour. After the separation of the catalyst by filtration, hydrochloric acid solution (10 mL, 5 N) was added to the filtrate solution, and the precipitated tetrazole was filtered and dissolved in hot ethanol. After the concentration of the solution, purification with column chromatography was carried out with the ethyl acetate: *n*-hexane eluent.

Spectroscopic data of the selected synthesized compounds

3-Phenyl-2-(1*H*-tetrazole-5-yl)acrylonitrile (6d). M.p. 166–169 °C; IR (KBr): ν_{max} = 3360, 3235, 3059, 2220, 1612, 1576, 1498 cm^{-1}. ^1H NMR (DMSO-d_6): δ = 3.54 (brs, –N*H*, overlap with solvent) 7.51–7.54 (m, 3H, Ar–H), 7.54–7.93 (m, 2H, Ar–H), 8.12 (s, 1H, CH) ppm; ^{13}C NMR (DMSO-d_6): δ = 103.3, 118.0, 129.4, 129.4, 130.7, 134.2, 141.0, 157.8 ppm.

3-(3-Methylphenyl)-2-(1*H*-tetrazole-5-yl) acrylonitrile (6f). M.p. 131–133 °C; IR (KBr): ν_{max} = 3509, 3177, 2925, 2221, 1615,

Table 4 Comparison of MMT-BAC@Cu(0) and DES with other catalysts and conditions used for the synthesis of 5-phenyl-1*H*-tetrazole

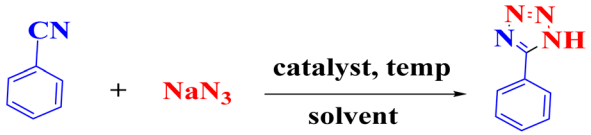

Entry	Catalyst	Condition	Time (h)	Yield[a] (%)	Ref.
1	Pd-adenine@boehmite	PEG, 120 °C	1.5	95	20
2	$(NH_4)Ce(NO_3)_6$	DMF, 110 °C	6	97	43
3	Fe_3O_4@SiO_2/aza-crown ether-Cu(II)	PEG-200, 100 °C	2.5	95	44
4	Cu(II)–NaY	DMF, 120 °C	3.5	99	45
5	$ZnCl_2$	H_2O, reflux	15	78	46
6	Cu-TBA@biochar	PEG, 130 °C	7	98	47
7	MMT-BAC@Cu(0)	DES: ChCl : urea (1 : 2), 80 °C	0.5	99	This work

[a] Isolated yield.

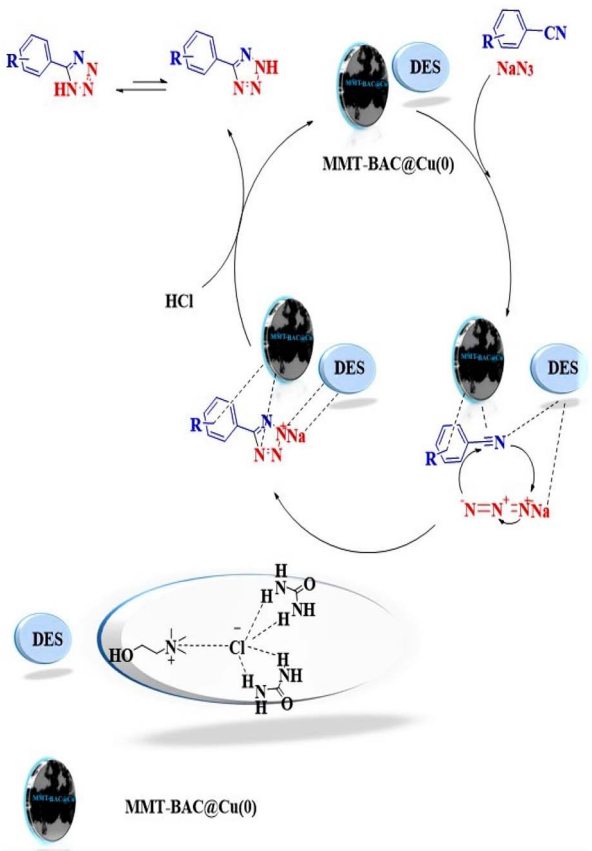

Fig. 8 Proposed mechanism for the synthesis of 5-substituted 1*H*-tetrazole derivatives.

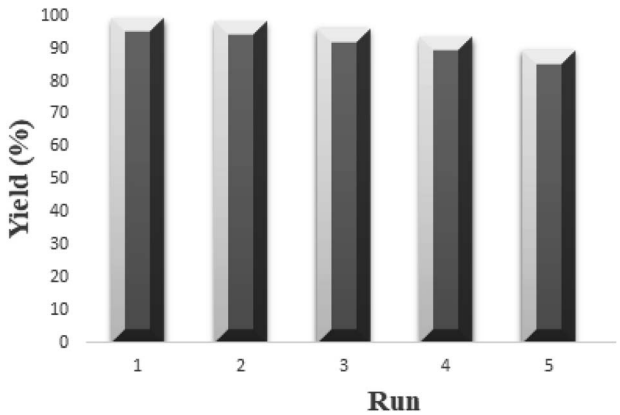

Fig. 9 Reusability of MMT-BAC@Cu(0) nanocatalyst.

1489 cm^{-1}. ^1H NMR (DMSO-d_6): δ = 2.38 (3H, s, CH_3); 3.54 (br. s, –N*H*, overlap with solvent signal), 7.29 (s, 1H, Ar–H), 7.37–7.73 (t, 1H, Ar–H); 7.74–7.77 (2H, m, Ar–H); 8.06 (1H, s, CH) ppm; ^{13}C NMR (DMSO-d_6): 21.4, 103.2, 118.1, 126.4, 129.3, 130.0, 131.4, 134.1, 138.6, 141.0, 157.8 ppm.

5-(4-Methylphenyl)-1*H*-tetrazole (5c). M.p. 250–251 °C; IR (KBr): ν_{max} = 3150, 2917, 2698, 1613, 1570, 1504, 1434, 1401, 1164, 823, 744, 698 cm^{-1}. ^1H NMR (DMSO-d_6): δ = 7.93 (d, 2H, Ar–H), 7.43 (d, 2H, Ar–H), 2.39 (s, 3H), tetrazole N*H* off-scale ppm.

5-(4-Chlorophenyl)-1*H*-tetrazole (5e). M.p. 260–261 °C; IR (KBr): ν_{max} = 3125, 2908, 2851, 1609, 1486, 1434.76, 1407, 1277, 1254, 1160, 1095, 1053, 881, 744, 693 cm^{-1}. ^1H NMR (DMSO-d_6): δ = 8.04 (d, 2H, Ar–H), 7.66 (d, 2H, Ar–H), 4.15 (brs, 1H,–N*H*) ppm.

Conclusion

In conclusion, we introduced an eco-friendly and efficient approach for the synthesis of 5-substituted 1*H*-tetrazole derivatives from raw materials of benzonitrile and sodium azide through the [2 + 3] cycloaddition reaction as well as 2-(1*H*-tetrazole-5-yl) acrylonitrile derivatives as the preferred product from raw materials of aldehyde, malononitrile, and sodium azide through multicomponent domino reactions (MDRs) in the presence of the MMT-BAC@Cu(0) nanoclay as a heterogeneous and green catalyst in DES as a green solvent. The MMT-BAC@Cu(0) nanocatalyst used benefits from properties such as high surface reactivity, biocompatibility, non-toxicity, and

inexpensiveness. Some advantages of the green solvent used in the study are non-flammability, high solubility, degradability, expensiveness, recyclability, and non-volatility. This method was proven to be more efficient than the previous methods, which employed hazardous organic solvents and toxic metals and performed the process with a longer reaction time. Using the proposed approach, the reaction was performed in a shorter time under green conditions with good to excellent efficiency and without the need for additional reagents. We hope that the presented method can be generalized in the future to synthesize heterocyclic derivatives with important biological properties to be used in valuable research projects by adhering to the principles of green chemistry.

Author contributions

Hossein Eshghi: conceptualization, methodology, data curation, investigation, supervising the work, review & editing. Fatemeh Pirani: methodology, data curation, investigation, writing-original draft. S. Amin Rounaghi: conceptualization, methodology, data curation, investigation.

Conflicts of interest

The authors declare that they have no known competing financial interests or personal relationships that could have appeared to influence the work reported in this paper.

Acknowledgements

The authors gratefully acknowledged for partial financial support of this study by Ferdowsi University of Mashhad (Grant No. 3/55292).

References

1 S. Z. Dalil Heirati, F. Shirini and A. Fallah Shojaei, *Res. Chem. Intermed.*, 2017, **43**, 6167–6186.
2 B. J. Borah, S. J. Borah, K. Saikia and D. K. Dutta, *Appl. Catal., A*, 2014, **469**, 350–356.
3 H. Wang, N. Wang, F. Wang, F. Xiao and D. Pan, *Sep. Purif. Technol.*, 2020, **251**, 117346.
4 J. Wang, Y. Chen, G. Liu and Y. Cao, *Composites, Part B*, 2017, **114**, 211–222.
5 B. Zeynizadeh and S. Rahmani, *RSC Adv.*, 2019, **9**, 28038–28052.
6 N. Y. Baran, T. Baran and A. Menteş, *Appl. Clay Sci.*, 2019, **181**, 105225.
7 S. Sadjadi, M. M. Heravi, M. Malmir and F. G. Kahangi, *Appl. Clay Sci.*, 2018, **162**, 192–203.
8 A. Mermer, T. Keles and Y. Sirin, *Bioorg. Chem.*, 2021, **114**, 105076.
9 S. Podha and F. R. Meeran, *World J. Biol. Pharm. Health Sci.*, 2022, **12**, 114–121.
10 J. Becker, C. Manske and S. Randl, *Curr. Opin. Green Sustainable Chem.*, 2022, **33**, 100562.
11 J. Maes, T. R. Rauws and B. U. Maes, *Chem.–Eur. J.*, 2013, **19**, 9137–9141.
12 M. N. Shaikh, M. A. Aziz, A. N. Kalanthoden, A. Helal, A. S. Hakeem and M. Bououdina, *Catal. Sci. Technol.*, 2018, **8**, 4709–4717.
13 F. Carpentier, F.-X. Felpin, F. Zammattio and E. Le Grognec, *Org. Process Res. Dev.*, 2020, **24**, 752–761.
14 Z. Hajizadeh, F. Hassanzadeh-Afruzi, D. F. Jelodar, M. R. Ahghari and A. Maleki, *RSC Adv.*, 2020, **10**, 26467–26478.
15 Z. N. Tisseh, M. Dabiri, M. Nobahar, H. R. Khavasi and A. Bazgir, *Tetrahedron*, 2012, **68**, 1769–1773.
16 P. Akbarzadeh, N. Koukabi and E. Kolvari, *Res. Chem. Intermed.*, 2019, **45**, 1009–1024.
17 J. Safaei-Ghomi and S. Paymard-Samani, *Chem. Heterocycl. Compd.*, 2015, **50**, 1567–1574.
18 N. Moeini, M. Ghadermazi and S. Molaei, *J. Mol. Struct.*, 2022, **1251**, 131982.
19 H. R. Pawar and R. C. Chikate, *J. Mol. Struct.*, 2021, **1225**, 128985.
20 B. Tahmasbi, A. Ghorbani-Choghamarani and P. Moradi, *New J. Chem.*, 2020, **44**, 3717–3727.
21 T. Tamoradi, B. Mehraban-Esfandiari, M. Ghadermazi and A. Ghorbani-Choghamarani, *Res. Chem. Intermed.*, 2018, **44**, 1363–1380.
22 M. S. Ghasemzadeh and B. Akhlaghinia, *ChemistrySelect*, 2020, **5**, 6440–6452.
23 M. Esmaeilpour, A. R. Sardarian and H. Firouzabadi, *Appl. Organomet. Chem.*, 2018, **32**, e4300.
24 M. N. Shaikh, M. A. Aziz and Z. H. Yamani, *Catal. Sci. Technol.*, 2020, **10**, 6544–6551.
25 M. N. Shaikh, M. M. Abdelnaby, A. S. Hakeem, G. A. Nasser and Z. H. Yamani, *ACS Appl. Nano Mater.*, 2021, **4**, 3508–3518.
26 S. Adeyeye Nafiu, S. Shaheen Shah, A. Aziz and M. N. Shaikh, *Chem.–Asian J.*, 2021, **16**, 1956–1966.
27 M. N. Shaikh and M. H. Zahir, *J. Organomet. Chem.*, 2022, 973–974.
28 D. Ge, L. Hu, J. Wang, X. Li, F. Qi, J. Lu, X. Cao and H. Gu, *ChemCatChem*, 2013, **5**, 2183–2186.
29 A. N. Kalanthoden, M. N. Shaikh, M. A. Aziz and S. K. Rani, *ChemistrySelect*, 2019, **4**, 12832–12840.
30 J. B. Zimmerman, P. T. Anastas, H. C. Erythropel and W. Leitner, *Science*, 2020, **367**, 397–400.
31 N. K. Ojha, G. V. Zyryanov, A. Majee, V. N. Charushin, O. N. Chupakhin and S. Santra, *Coord. Chem. Rev.*, 2017, **353**, 1–57.
32 S. T. Fardood, A. Ramazani and S. Moradi, *J. Sol-Gel Sci. Technol.*, 2017, **82**, 432–439.
33 M. Nasrollahzadeh, N. Motahharifar, Z. Nezafat and M. Shokouhimehr, *Colloid Interface Sci. Commun.*, 2021, **44**, 100471.
34 E. Valiey and M. G. Dekamin, *Sci. Rep.*, 2022, **12**, 18139.
35 V. Khorramabadi, D. Habibi and S. Heydari, *Green Chem. Lett. Rev.*, 2020, **13**, 50–59.
36 Y. Rangraz, F. Nemati and A. Elhampour, *Ind. Eng. Chem. Res.*, 2019, **58**, 17308–17318.

37 B. Zeynizadeh, S. Rahmani and H. Tizhoush, *Polyhedron*, 2020, **175**, 114201.
38 M. S. Alhumaimess, A. A. Essawy, M. M. Kamel, I. H. Alsohaimi and H. M. Hassan, *Nanomaterials*, 2020, **10**, 781.
39 R. Phul, C. Kaur, U. Farooq and T. Ahmad, *Mater. Sci. Eng Int. J.*, 2018, **2**, 90–94.
40 F. Pourhassan and H. Eshghi, *Catal. Lett.*, 2020, **150**, 1287–1300.
41 Y. Liu, X. Qi, W. Zhang, P. Yin, Z. Cai and Q. Zhang, *Org. Lett.*, 2020, **23**, 734–738.
42 M. Bakherad, R. Doosti, A. Keivanloo, M. Gholizadeh and K. Jadidi, *J. Iran. Chem. Soc.*, 2017, **14**, 2591–2597.
43 S. Kumar, S. Dubey, N. Saxena and S. K. Awasthi, *Tetrahedron Lett.*, 2014, **55**, 6034–6038.
44 F. Rezaei, M. A. Amrollahi and R. Khalifeh, *Inorg. Chim. Acta*, 2019, **489**, 8–18.
45 K. Sudhakar, B. P. Chandra Rao, B. P. Kumar, M. Suresh and S. Ravi, *Asian J. Chem.*, 2017, **29**, 864–866.
46 A. Saeed, M. Hussain and M. Qasim, *Turk. J. Chem.*, 2014, **38**, 436–442.
47 P. Moradi, M. Hajjami and B. Tahmasbi, *Polyhedron*, 2020, **175**, 114169.
48 A. Abbott, G. Capper, D. Davies and R. Rasheed, *Chem. Commun.*, 2003, **10**, 70–71.